FAR-FROM-EQUILIBRIUM ATTRACTORS IN A 3+1D TRANSPORT APPROACH AT FIXED η/s*

Salvatore Plumari[a,b], Giuseppe Galesi[a,b], Lucia Oliva[a,c]
Vincenzo Nugara[a,b], Vincenzo Greco[a,b]

[a]Department of Physics and Astronomy "E. Majorana", University of Catania
Via S. Sofia 64, 95125 Catania, Italy
[b]Laboratori Nazionali del Sud, INFN-LNS, Via S. Sofia 62, 95123 Catania, Italy
[c]INFN Sezione di Catania, Via S. Sofia 64, 95123 Catania, Italy

Received 1 August 2022, accepted 21 August 2022,
published online 14 December 2022

We investigate the existence of far-from-equilibrium attractors in moments of the one-particle distribution function within the framework of a 3+1D Boltzmann transport approach at fixed η/s. We compare our results for a conformal and non-conformal gas for different values of η/s and different initial anisotropy.

DOI:10.5506/APhysPolBSupp.16.1-A27

1. Introduction

In recent years, viscous hydrodynamics approaches have been successful in describing experimental data of ultra-relativistic heavy-ion collisions (URHICs): hadron p_{T}-spectra and anisotropic flows [1]. In recent years, collective behavior like those observed in heavy-ion collisions has been also observed in small collision systems. All these experimental results have raised the question whether the QGP has been created in these small systems. Recent theoretical calculations based on hydrodynamical simulations have been successful in describing data when the system is far from equilibrium which is outside their region of applicability. Therefore, understanding the thermalization of systems which are far from equilibrium is of fundamental importance in the context of URHICs. This necessity becomes increasingly important in the case of small collision systems like the one produced in pp and pA collisions, where matter most likely remains far from equilibrium throughout its dynamical evolution. On the other hand, in recent years,

* Presented at the 29$^{\mathrm{th}}$ International Conference on Ultrarelativistic Nucleus–Nucleus Collisions: Quark Matter 2022, Kraków, Poland, 4–10 April, 2022.

it has been found by different models including AdS/CFT simulations, kinetic theory in Relaxation Time approximation (RTA) or QCD-based kinetic approaches that the dynamics show a universal behavior (denoted as non-equilibrium attractor) which is possible to describe by viscous hydrodynamics in a finite time [2–7].

In these proceedings, we discuss the existence of non-equilibrium attractors considering the behavior of general moments of the one-particle distribution function in the case of conformal and non-conformal systems within a Relativistic Boltzmann Transport approach.

2. Relativistic Boltzmann Transport

In this work we have employed the Relativistic Boltzmann Transport (RBT) approach developed recently to perform studies of the quark–gluon plasma dynamics in uRHICs for different systems from RHIC to LHC energies [8–16]. In our approach, we describe QGP matter with an on-shell one-particle distribution function f, depending on space-time coordinates $x^\mu = (t, \boldsymbol{x})$ and 3-momentum $\boldsymbol{p}$. The space-time evolution of f is governed by the following Relativistic Boltzmann Transport (RBT) equation

$$\left(p^\mu \partial_\mu + \frac{1}{2}\partial_i m^2 \partial^i_{(p)}\right) f_1 = C\left[f\right]_{\boldsymbol{p}} \, , \tag{1}$$

where $p^0 = E_{\boldsymbol{p}} \equiv \sqrt{m^2 + \boldsymbol{p}^2}$, $\partial_\mu \equiv \partial/\partial x^\mu$, and $\partial^i_{(p)} \equiv -\partial/\partial p^i$. The quantity $C\left[f\right]_{\boldsymbol{p}}$ is the collision integral which, considering only binary collisions as we do in this work, is given by

$$C\left[f\right]_{\boldsymbol{p}} = \int\limits_{2}\int\limits_{1'}\int\limits_{2'} \left(f_{1'} f_{2'} - f_1 f_2\right) |\mathcal{M}|^2 \, \delta^{(4)}\left(p_1 + p_2 - p_{1'} - p_{2'}\right) \, , \tag{2}$$

with $\int_k = \int \frac{\mathrm{d}^3 p_k}{2E_{\boldsymbol{p}_k}(2\pi)^3}$ and $\mathcal{M}$ denoting the transition amplitude for the elastic processes which is directly linked to the differential cross section $|\mathcal{M}|^2 = 16\pi\, s\,(s{-}4M^2)\mathrm{d}\sigma/\mathrm{d}t$ with s the Mandelstam-invariant. In our calculations, the viscosity is fixed by determining the total isotropic cross section according to the Chapman–Enskog approximation, for details see [17].

3. Results

We have employed the RBT to perform a study of the existence of far-from-equilibrium attractors in the moments of the one-particle distribution function. We have considered a system undergoing one-dimensional Bjorken expansion in two different cases: the conformal limit where $m = 0$ and the non-conformal limit corresponding to an equation of state of massive particles $m \neq 0$.

In our calculations, the initial pressure anisotropy is modeled by setting the initial phase-space distribution function f_0 to be equal to the spheroidally deformed thermal initial conditions referred to as Romatschke–Strickland distribution for the ideal gas [18]

$$f_0 = \frac{g}{(2\pi)^3} \exp\left[-\frac{1}{\Lambda_0}\sqrt{\sum_i \frac{p_i^2}{\alpha_i} + m^2}\right], \tag{3}$$

where the parameter Λ_0 corresponds to an effective initial temperature parameter that sets the magnitude of the initial energy density. In our calculation, Λ_0 is fixed in order to have the initial energy density corresponding to a gas with mass m at a temperature $T = 0.5$ GeV. In the results shown in this paper, the parameters α_i are fixed in the following way: $\alpha_x = \alpha_y = 1$ and α_z is a free parameter chosen in order to fix the initial longitudinal to transverse pressure ratio $P_{\mathrm{L}}/P_{\mathrm{T}}$. The isotropic Boltzmann distribution is recovered with $\alpha_x = \alpha_y = \alpha_z = 1$, and in this limit, the parameter Λ_0 is the usual initial temperature. In all the calculations shown in this paper, we have considered a 1+1D expanding medium which is obtained considering an expanding cylinder in the longitudinal direction and where we impose periodic boundary conditions in the transverse plane.

Firstly, we present results for the time evolution of $P_{\mathrm{L}}/P_{\mathrm{T}}$ ratio for a gas of massless particles for different anisotropic initial conditions in the momentum distribution and in a range of η/s explored in uRHIC's. In Fig. 1, it is shown the $P_{\mathrm{L}}/P_{\mathrm{T}}$ evaluated at mid-rapidity and as a function of proper time scaled by the typical interaction time $\tau_{\mathrm{R}} \equiv 4\pi\,(\eta/s)\,/T\,(\tau)$. Notice that here T is the effective temperature calculated from the energy density. As shown, we observe a rapid information loss of the initial condition leading to a universal behavior in ~ 3, 4 particle collisions. Independently of the initial anisotropy of the system, all curves converge on a unique attractor, as observed in other works [2, 3].

In a systematic way, we can perform a similar calculation that has been proposed in [7]. In a similar way, we define a general set of moments in kinetic theory related to the distribution function for on-shell particles given by

$$\mathcal{M}^{mn}(\tau) = \int \frac{\mathrm{d}^3 p}{(2\pi)^3} p^{n-1} p_z^{2m} f(\tau, p)\,, \tag{4}$$

where one can reduce powers of the energy and powers of the longitudinal momentum. The study of all the moments in 1D can encode all the information of the distribution function. Following Ref. [7], the moments will be scaled by their corresponding equilibrium values $\mathcal{M}^{mn}_{\mathrm{eq}} = T^{n+2m+2}\Gamma(n+2m+2)\zeta(n+2m+2)/[2\pi^2(2m+1)]$, where T is the temperature.

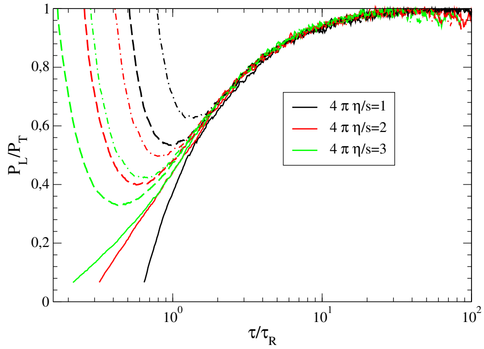

Fig. 1. $P_{\rm L}/P_{\rm T}$ as a function of the scaled time $\tau/\tau_{\rm R}$ for massless particles. Different curves correspond to different initial anisotropies and different η/s ratios.

Different moments probe different regions of the phase-space distribution function. In particular, larger moments give information about the high momentum part of the phase-space distribution function. In Fig. 2, it is shown the time evolution of the scaled moments $\mathcal{M}^{01}/\mathcal{M}^{01}_{\rm eq}$ and $\mathcal{M}^{21}/\mathcal{M}^{21}_{\rm eq}$. Notice that $\mathcal{M}^{01}/\mathcal{M}^{01}_{\rm eq} = P_{\rm L}/P_{\rm L,eq}$, where $P_{\rm L,eq}$ is the longitudinal pressure at the equilibrium. Different lines refer to different initial values of $P_{\rm L}/P_{\rm L,eq}$ which in our choice of the distribution function, correspond to different momentum anisotropy parameter α_z. As shown in Fig. 2, the evolution of all the various different initial conditions eventually approaches a universal curve that corresponds to the late-time attractor similar to that observed by other models [2, 4–7]. Comparing the universal curve where all the calculations collapse, which is the solution of the attractor with the attractor obtained in viscous hydrodynamics framework and shown by solid smooth (blue) curve,

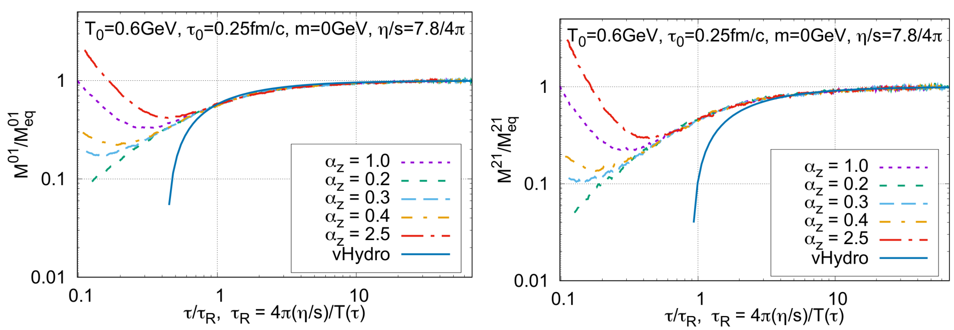

Fig. 2. (Color online) Time evolution of the scaled moments $\mathcal{M}^{01}$ (left panel) and $\mathcal{M}^{21}$ (right panel). Different colors refer to different initial longitudinal anisotropic parameter values that we have fixed to the following values α_z = 0.2, 0.3, 0.4, 1.0, 2.5. The solid smooth (blue) line is the vHydro attractor [19].

we observe that for low moments, the kinetic attractor is well described by viscous hydrodynamics already for $\tau/\tau_{\mathrm{R}} \sim 0.8$. On the other hand, for higher moments, we can see that the kinetic attractor approaches the solid smooth (blue) curve at a later time $\tau/\tau_{\mathrm{R}} \geq 3$. This suggests that particle with larger momenta need larger time to reach the equilibrium and this is related to the fact that higher moments approach the solid smooth (blue) curve later.

Finally, in Fig. 3, we have shown the $P_{\mathrm{L}}/P_{\mathrm{T}}$ ratio for the massive case at mid-rapidity and for $\eta/s = 1/(4\pi)$. We observe that for $\tau/\tau_{\mathrm{R}} \leq 2$ different calculations with different masses and corresponding to different initial anisotropic parameters approach the universal attractor.

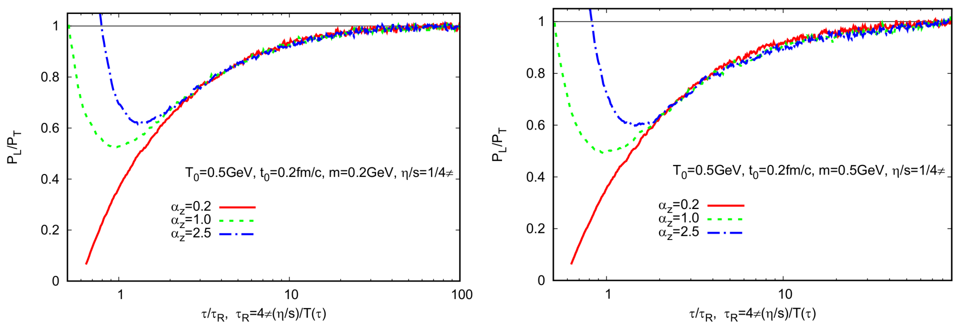

Fig. 3. $P_{\mathrm{L}}/P_{\mathrm{T}}$ as a function of the scaled time τ/τ_{R} for $m = 0.2$ GeV (left panel) and $m = 0.5$ GeV (right panel). Different curves correspond to different initial anisotropic parameters. In these calculations, $\eta/s = 1/(4\pi)$.

4. Conclusion

We have investigated the existence of far-from-equilibrium attractors within the framework of a 3+1D Boltzmann transport approach at fixed η/s. We have shown results for conformal and non-conformal gas and for different initial anisotropies and different η/s ratios. In the conformal limit, we have studied the moments decomposition of the distribution function introduced in Ref. [7]. We observe that for the moments considered, our solution converges to the attractor solution at a finite time: higher moments approach slower the viscous hydrodynamical attractor for $\tau \sim 3\tau_{\mathrm{R}}$ while lower moments faster in $\tau \sim \tau_{\mathrm{R}}$. This suggests that the distribution function should show an attractor-like behavior.

REFERENCES

[1] M. Alqahtani, M. Nopoush, R. Ryblewski, M. Strickland, *Phys. Rev. C* **96**, 044910 (2017).

[2] M.P. Heller, M. Spaliński, *Phys. Rev. Lett.* **115**, 072501 (2015).

[3] A. Behtash, C.N. Cruz-Camacho, M. Martinez, *Phys. Rev. D* **97**, 044041 (2018).

[4] M. Spaliński, *Phys. Lett. B* **776**, 468 (2018).

[5] M. Strickland, *J. High Energy Phys.* **1812**, 128 (2018).

[6] A. Kurkela, W. van der Schee, U.A. Wiedemann, B. Wu, *Phys. Rev. Lett.* **124**, 102301 (2020).

[7] D. Almaalol, A. Kurkela, M. Strickland, *Phys. Rev. Lett.* **125**, 122302 (2020).

[8] S. Plumari, A. Puglisi, F. Scardina, V. Greco, *Phys. Rev. C* **86**, 054902 (2012).

[9] F. Scardina, M. Colonna, S. Plumari, V. Greco, *Phys. Lett. B* **724**, 296 (2013).

[10] F. Scardina *et al.*, *Phys. Rev. C* **90**, 054904 (2014).

[11] M. Ruggieri *et al.*, *Phys. Rev. C* **92**, 064904 (2015).

[12] S.K. Das *et al.*, *J. Phys. G: Nucl. Part. Phys.* **44**, 095102 (2017).

[13] F. Scardina *et al.*, *Phys. Rev. C* **96**, 044905 (2017).

[14] Y. Sun, S. Plumari, V. Greco, *Eur. Phys. J. C* **80**, 16 (2020).

[15] M.L. Sambataro, S. Plumari, V. Greco, *Eur. Phys. J. C* **80**, 1140 (2020).

[16] A. Gabbana *et al.*, *Phys. Rev. C* **101**, 064904 (2020).

[17] S. Plumari, G.L. Guardo, F. Scardina, V. Greco, *Phys. Rev. C* **92**, 054902 (2015).

[18] P. Romatschke, M. Strickland, *Phys. Rev. D* **68**, 036004 (2003).

[19] G.S. Denicol, T. Koide, D.H. Rischke, *Phys. Rev. Lett.* **105**, 162501 (2010).